Mapping Attosecond Electron Wave Packet Motion

Hiromichi Niikura,[1,2,*] D. M. Villeneuve,[1] and P. B. Corkum[1]

[1]National Research Council of Canada 100 Sussex Drive, Ottawa, Ontario, Canada K1A0R6
[2]PRESTO, Japan Science and Technology Agency, 4-1-8 Honcho Kawaguchi, Saitama, Japan.

(Received 23 July 2004; published 2 March 2005)

Attosecond pulses are produced when an intense infrared laser pulse induces a dipole interaction between a sublaser cycle recollision electron wave packet and the remaining coherently related bound-state population. By solving the time-dependent Schrödinger equation we show that, if the recollision electron is extracted from one or more electronic states that contribute to the bound-state wave packet, then the spectrum of the attosecond pulse is modulated depending on the relative motion of the continuum and bound wave packets. When the internal electron and recollision electron wave packet counterpropagate, the radiation intensity is lower. We show that we can fully characterize the attosecond bound-state wave packet dynamics. We demonstrate that electron motion from a two-level molecule with an energy difference of 14 eV, corresponding to a period of 290 asec, can be resolved.

DOI: 10.1103/PhysRevLett.94.083003 PACS numbers: 33.80.Rv, 42.50.Hz

One of the aims of attosecond science is to observe single or multielectron dynamics [1–5]. Recently, two types of multielectron dynamics have been observed. One is the Auger ionization dynamics excited by a single photon extreme ultraviolet laser pulse with a $\sim$1 fs pulse duration [2]. The Auger electron is streaked by a delayed, intense laser pulse that probes the time when the Auger electron is released from the atom. The other is recollision electron dynamics during intense field ionization [4,5]. The vibrational wave packet motion of H_2^+ produced simultaneously with the electron wave packet clocks the time of emission of the secondary electron as well as the time of recollision of the primary electron. However, in both cases, the electron that has been observed is in the continuum. A method to observe attosecond single or multielectron dynamics in a bound potential has not been established.

We present a method of probing *internal* single electron wave packet motion based on unique characteristics of attosecond technology. Attosecond optical pulses are generated by a coherent interaction between a recollision wave packet and the bound-state electron wave function or wave packet from which it was created [6]. Thus the optical pulse that is generated is really a probe of this interaction. We show that, when an internal electron wave packet is formed, the wave packet motion is mapped onto the attosecond spectrum. We also show that, although the bound-state wave packet is composed of two or more stationary states, the continuum electron can tunnel from any stationary state that contributes to the wave packet and still the full *wave packet dynamics can be probed*. In fact, the interpretation is easiest if the electron tunnels from a single stationary state.

In our approach, time resolution can be achieved by one of two methods. Either one can use pump-probe techniques similar to those used in many ultrafast experiments: a pump pulse initiates wave packet motion and a probe pulse follows its evolution by producing the attosecond optical pulse. Wave packet motion is revealed in the dependence of any spectral component of the attosecond pulse as a function of the pump-probe delay time. Or one can make a single-shot measurement: the amplitude of the spectrum of a single attosecond pulse records the full attosecond bound-state wave packet dynamics. The spectrum of the attosecond pulse is modulated with a period that is determined by the interplay between the chirp of the continuum electron and the motion of the bound electron wave packet. In either case, when the recollision and bound-state electron wave packets copropagate, the spectrum component emitted at that time is slightly enhanced. If they counterpropagate, the corresponding component is suppressed.

For our simulation, an initial wave packet, $\psi(t)$, is prepared as a coherent sum of two electronic wave functions with an initial phase, ϕ: $\psi(t) = \psi_0 + \psi_1 \times \exp[-i(\Delta E\, t/\hbar + \phi)]$, where ψ_n are field-free wave functions, and ΔE is the energy separation between them [7]. Solving the 1D time-dependent Schrödinger equation, we calculate the time evolution of the electron wave packet in the presence of the laser field, $E(t)$. In a 1D model, the multiple recollision and overall recollision probability might be overestimated compared to a 3D model. However, in the case of a few-cycle laser pulse, that effect should be small. The spectrum of high harmonic radiation is given by a Fourier transform of the expectation value of the dipole acceleration, $\ddot{d}(t) = \langle\psi(t)|dV/dx + eE(t)|\psi(t)\rangle$ [8].

We use a doubly charged ion and a single electron. The total Hamiltonian is given by $H = T + V + eE(t)x$, where T and V are the kinetic energy and potential energy operators, and x is the coordinate. We use a two-center potential to give us control of the level spacing and ionization potential: $V = -1/\sqrt{(x - R/2)^2 + a^2} - 1/\sqrt{(x + R/2)^2 + a^2}$, where a is a smoothing parameter, and R is the internuclear distance between two nuclei [9].

We adjust the values of a and R to change the energy levels and therefore the period of the wave packet motion.

We assume a laser pulse with a wavelength of 1600 nm. We choose 1600 nm instead of 800 nm because the longer wavelength minimizes nonadiabatic effect associated with ionization or excitation [10,11] and also ensures that the peak recollision energy is large. To give predominantly one recollision during a laser pulse, the carrier-envelope phase is adjusted, $E(t) = \sin[\omega(t - t_0)]\exp[-(t - t_0)^2/2\sigma^2]$, where $t_0 = 8$ fs and $\sigma = 6/\sqrt{8\ln 2}$ fs. Although the wavelength that we assume is longer than used in current phase stabilized experiments [12], our pulse is otherwise experimentally realistic; optical-parametric chirped-pulse amplification techniques will make phase controlled 1600 nm pulses experimentally accessible soon [13].

The kinetic energy of the recollision electron and hence the extreme ultraviolet radiation frequency that it produces is uniquely mapped to time [14]. The electron kinetic energy generally chirps first up to $3.17U_p + 1.32I_p$, where U_p is the pondermotive energy, then down again over $\sim 1/3$ of the optical period. In the case of a few-cycle laser pulse with fixed carrier-envelope phase, the cutoff energy is slightly lower due to the rapidly decreasing envelope. The same electron kinetic energy occurs twice per half period—the first is called the short trajectory, the second is called the long trajectory. We choose the pulse duration and carrier-envelope phase so that only the short trajectory contributes to the plateau region of high harmonic radiation. Even with a longer laser pulse, the short trajectory can be selected experimentally [14,15].

Figure 1 plots the high harmonic spectra for three different bound-state electronic wave packets prepared from an equal population of the ground and first excited state at $t = 0$ and $\phi = 0$. In this case, the electron wave packet oscillates from side to side in the potential. The laser intensity is 10^{14} W/cm^2.

Figure 1(a) shows the spectrum for $\Delta E = 14.2$ eV (solid line) ($R = 0.4$ Å and $a = 0.65$ Å). The vertical ionization energy is 32.8 eV for the ground and 18.6 eV for the first excited state. The period of the electron wave packet is 290 asec. The dominant peak appearing at 14 eV is due to the dipole interaction in the bound-state wave packet motion itself. Note that, due to the short pulse duration, no harmonics separated by $2\omega(= 1.55$ eV) appear [12]. However, the spectrum shows periodic intensity dips that reflect the interaction between the motion of the bound state and recollision electron wave packets.

For reference we also show the spectrum where only the excited state is populated and thus there is no wave packet motion (dotted line). In this case there are no dips in the spectrum. Comparing the two, we see that the spectrum with both states populated extends to higher energy by ΔE than when only the excited state is populated.

The number of dips in the spectrum decreases when the electron wave packet moves more slowly. Figures 1(b) and 1(c) plot the spectrum for different values of R and a [0.4 Å and 0.75 Å for Fig. 1(b) and 0.3 Å and 0.9 Å for Fig. 1(c)]. The period of the electron motion is 330 asec and 444 asec, respectively. The energy of the ground and excited state is 28.8 eV and 16.8 eV for Fig. 1(b), and 24.2 eV and 14.9 eV for Fig. 1(c), thus ΔE is 12 eV and 9.3 eV. At 10^{14} W/cm^2, only 1% of the population tunnels from the excited state to the ionization continuum in Fig. 1(a), compared with 10% [in Fig. 1(b)] and 50% [in Fig. 1(c)]. In each case, the ground state does not ionize. Depletion of the excited state causes the spectrum to become shallower.

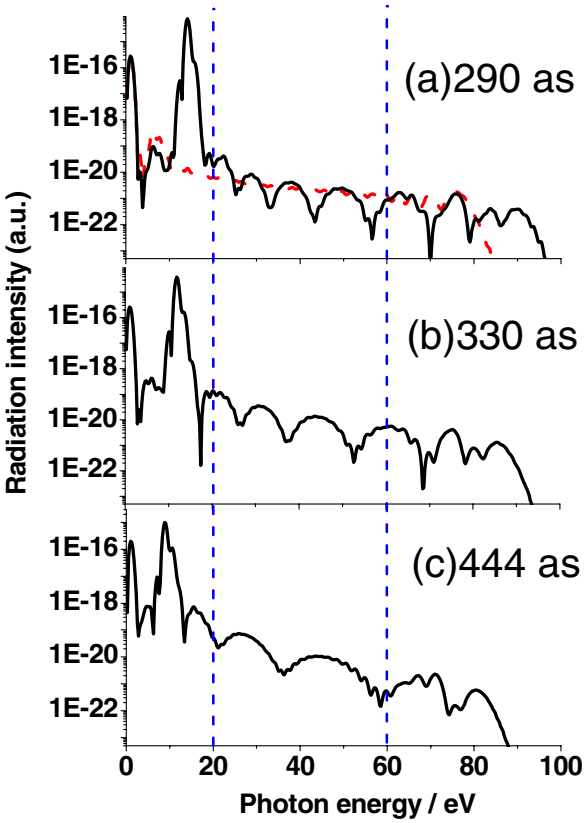

FIG. 1 (color online). Shows the calculated high harmonic spectra from a bound-state electron wave packet with a period of (a) 290 asec, (b) 330 asec, and (c) 444 asec. The initial wave packet is prepared by a superposition of field-free ground and excited state wave functions. The laser pulse is 1600 nm, 10^{14} W/cm^2, 6 fs FWHM. The carrier-envelope phase is fixed (see text). Compared to when only the excited state is populated [dotted line in (a)], the spectra have periodic intensity dips that show the attosecond wave packet motion. As the motion becomes slower, the modulation period decreases.

We now concentrate on the physical origin of the spectral modulation. Figure 2 shows the relation between spectrum and time. The expectation value of the dipole acceleration is plotted in the left panel, and corresponding spectrum [Fourier transform of $\ddot{d}(t)$] is shown in the bottom. The solid line in the middle panel Fig. 2(b) plots the frequency chirp that is obtained by determining the instant

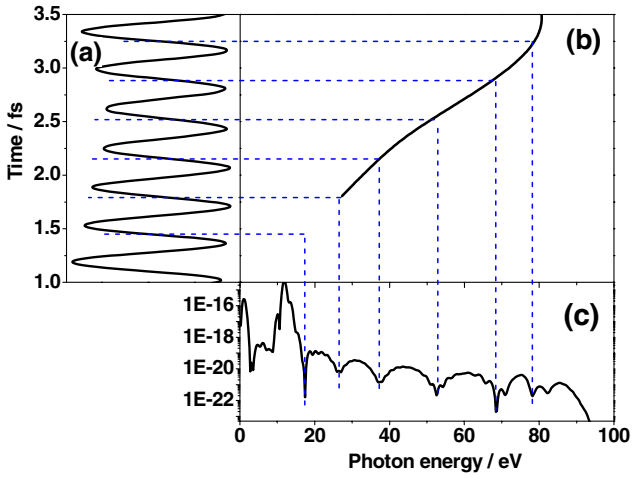

FIG. 2 (color online). Shows the relationship between photon energy and emission time: (a) time evolution of the dipole acceleration, (b) time-energy relation curve, and (c) the emitted spectrum. The conditions are the same as Fig. 1(b). The spectral intensity is suppressed when the dipole acceleration crosses zero from its positive side (dotted lines). It suggests that at those instants when the bound and recollision electron wave packets counterpropagate, the radiation intensity is lower.

of time at which each frequency is emitted [8,14]. The radiation energy increases until ~3.4 fs and then decreases. As seen from dotted lines in Fig. 2, the spectral intensity has a dip when the dipole acceleration, which is the second derivative of the position of the electron wave packet, crosses zero from its positive side. The spectral intensity is suppressed at those times when the bound and recollision electron wave packets counterpropagate. Thus, we see that the minima in the harmonic spectra correspond to motion of the internal electron wave packet.

The symmetry of the bound-state wave packet determines the form of the spectral modulation. As an example, we assume a symmetric wave packet formed from the ground and second excited state. This wave packet expands or shrinks with a period determined by ΔE. By evaluating the dipole moment, $d(t) = \langle\psi|ex|\psi\rangle$ analytically, we now show that the spectral intensity dips when the electron wave packet shrinks.

The total wave function, Ψ, is given by $\Psi = \psi_0 + \psi_1 \exp(-i\,\omega_{01}t) + \exp[-ikx - i\omega(t)\,t]$, where k is the wave number, $\omega(t)$ is the time-dependent angular frequency of the electron wave function in the continuum, and $\omega_{01} = \Delta E/\hbar$ is the angular frequency of the bound-state electron wave packet. Taking only the bound-continuum interaction, we obtain $\mathrm{d}(t) \propto A\cos(\omega t) - B\sin(\omega t) + C\cos(\omega - \omega_{01})t - D\sin(\omega - \omega_{01})t$, where $A = \int \psi_0 x\cos(kx)dx$, $B = \int \psi_0 x\sin(kx)dx$, $C = \int \psi_1\cos(kx)dx$, and $D = \int \psi_1 x\sin(kx)dx$. These integrals simplify if the symmetry of the ψ_0 and ψ_1 is known. If ψ_0 and ψ_1 are even functions, A and C are zero. In case of $\psi_0 \propto \exp(-x^2/2)$ and $\psi_n \propto (4x^2 - 2)\exp(-x^2/2)$, the modulation period is given by $\sim\sin[(2\omega - \omega_{01})t/2] \times \cos[-\omega_{01}t/2]$. When $\omega_{01}t = (2n - 1)$, where n is an integer, the dipole moment minimizes, leading to intensity dips in the spectrum.

We have shown how a bound-state wave packet can be observed in a single shot using the chirped recollision electron. Bound-state dynamics can also be measured by pump-probe techniques. Figure 3(a) plots the spectrum of an attosecond pulse produced by an 800 nm, 3 fs duration pulse. 3 fs is a bit shorter than any 800 nm pulse produced so far, but time-dependent polarization gives an alternative route [16] for achieving the effect that we calculate here. All other conditions are the same as Fig. 1(b).

Although the recollision energy is much smaller than with 1600 nm and therefore only a single dip appears in the spectrum of the attosecond pulse in Fig. 3(a), we now show that bound-state electron wave packet motion can still be measured. For the measurement, we choose a photon energy from the spectrum and observe its modulation. Figure 3(b) plots the spectral intensity at ~34 eV as a function of the initial phase of the electron wave packet, ϕ. Changing the initial phase corresponds to changing the delay between pump and probe. As the initial phase

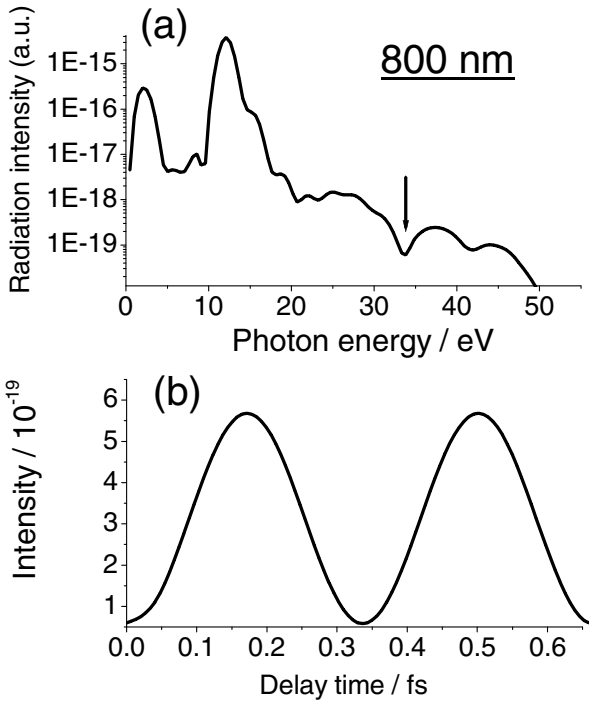

FIG. 3. (a) Plots the attosecond spectrum with a laser wavelength of 800 nm and 3 fs pulse duration. Other conditions are the same as Fig. 1(b). Only a single dip appears due to the smaller recollision energy compared with 1600 nm. (b) The spectral intensity at ~34 eV [the position is indicated by an arrow in (a)] as a function of the initial phase, ϕ, of the electron wave packet. In any spectral component, the intensity is modulated with a period of 330 asec.

changes, the intensity also changes. Each $\phi = 2\pi$ (330 as) the signal reproduces. This 330 asec modulation is seen across the spectrum.

We have shown that wave packet motion can be measured with time resolution approaching 100 asec and that wave packets whose periods differ by $\sim$10 asec can be distinguished (Fig. 1). Although we concentrated on using the recollision electron for the measurement, we stress that, since the strength of the attosecond emission is determined by the transition moment, the same information is contained in the photoelectron spectrum produced by an attosecond probe pulse. Together these two methods provide a very powerful new tool for attosecond measurements. However, measurement is only one part of an experiment. We must choose a dynamical process that is interesting to study, and determine how to excite it.

A coherent superposition of two electronic states can be prepared by resonant optical excitation [17], thereby inducing electron motion. The phase of the field oscillation of the exciting radiation determines the phase of the electronic wave packet. Thus, attosecond bound-state wave packets formed by two coherent states (very similar to those that we have assumed) can be produced now. Even this would be an important experiment since dynamics and imaging [18] could be combined in a single experiment. Looking further ahead, other approaches to attosecond wave packet formation that use high power attosecond pulses or shakeup [19] seem accessible.

The decay of a single electron wave packet probes the time evolution of the population or the coherence of the electronic states that compose the bound-state wave packet. Loss of coherence can occur, for example, through electron-vibrational coupling or electron-electron coupling. Loss of coherence is observed in the decay of the depth of modulation in the attosecond spectrum. Thus a single electron measurement can probe two-electron dynamics.

Although it is not obvious what determines the limit of time resolution of our method, we draw the reader's attention to the importance of measuring orbital relaxation and electron rearrangement following x-ray core ionization [20]. This occurs on a time scale of $<10^{-17}$ s. Rearrangement of the electronic wave function induces a multielectron internal electron wave packet as a precursor to Auger electron ejection. In the future, it should be possible to apply a short x-ray pump pulse inside one optical cycle of the infrared probe pulse. Then the recollision electron leaves an unperturbed atom and returns to probe its internal electron motion. Such an experiment, while well in the future, may be realized with the x-ray free-electron laser that is currently under development [21].

The authors acknowledge financial support from the National Science and Engineering Research Council, Photonic Research Ontario, Canadian Institute for Photonic Innovation, and Japan Society for the Promotion of Science.

*Electronic address: Hiromichi.Niikura@nrc.ca

[1] M. Hentshel *et al.*, Nature (London) **414**, 509 (2001).
[2] M. Drescher *et al.*, Nature (London) **419**, 803 (2002).
[3] R. Kienberger *et al.*, Nature (London) **427**, 817 (2004).
[4] H. Niikura *et al.*, Nature (London) **417**, 917 (2002).
[5] H. Niikura *et al.*, Nature (London) **421**, 826 (2003).
[6] M. Lewenstein, P. Balcou, M. Yu. Ivanov, A. L'Huillier, and P. B. Corkum, Phys. Rev. A **49**, 2117 (1994).
[7] A. Sanpera, J. B. Watson, M. Lewenstein, and K. Burnett, Phys. Rev. A **54**, 4320 (1996).
[8] K. Burnett, V. C. Reed, J. Cooper, and P. L. Knight, Phys. Rev. A **45**, 3347 (1992).
[9] T. Seideman, M. Yu. Ivanov, and P. B. Corkum, Phys. Rev. Lett. **75**, 2819 (1995).
[10] V. R. Bhardwaj, P. B. Corkum, and D. M. Rayner, Phys. Rev. Lett. **93**, 043001 (2004).
[11] A. N. Markevitch *et al.*, Phys. Rev. A **68**, 011402 (2003).
[12] A. Baltuška *et al.*, Nature (London) **421**, 611 (2003).
[13] X. Fang and T. Kobayashi, Opt. Lett. **29**, 1282 (2004).
[14] Y. Mairesse *et al.*, Science **302**, 1540 (2003).
[15] S. Salières, A. L'Huillier, and M. Lewenstein, Phys. Rev. Lett. **74**, 3776 (1996).
[16] M. Yu. Ivanov, P. B. Corkum, T. Zuo, and A. D. Bandrauk, Phys. Rev. Lett. **74**, 2933 (1995).
[17] M. Grønager and N. Henriksen, Chem. Phys. Lett. **278**, 166 (1997).
[18] J. Itatani *et al.*, Nature (London) **432**, 867 (2004).
[19] I. Litvinyuk *et al.* Phys. Rev. Lett. **94**, 033003 (2005).
[20] L. Hedin and G. Johansson, J. Phys. B **2**, 1336 (1969).
[21] A. Zholents and W. M. Fawley, Phys. Rev. Lett. **92**, 224801 (2004).